Staphylococcus aureus prophages are gatekeepers of exogenous lipid utilization to control membrane flexibility and bacterial fitness

Byang Zhou[a], Amit Pathania[a], Deepak Pant[a], Philippe Gaudu[a], Patrick Trieu-Cuot[b], Alexandra Gruss[a] and Karine Gloux[a].

[a]Université Paris-Saclay, INRAE, AgroParisTech, Micalis Institute, Jouy en Josas, France,

[b] Institut Pasteur, Université de Paris, CNRS UMR 2001, Unité de Biologie des Bactéries Pathogènes à Gram-Positif, Paris Cedex 15, France.

For correspondence: karine.gloux@inrae.fr

Key words: triglycerides, diglycerides, sphingomyelins, FASII, bacteriophage, Geh lipase, Hlb hemolysin B, FakB1.

Significance

Staphylococcus aureus is a major human health challenge. Its lipases activities are crucial for virulence and immune response escape. Prophages inserted in lipases are common in *S. aureus* but the selective benefits of their maintenance is little understood. We demonstrate that two prophages, inserted in triglyceride and sphingomyelin lipase genes, interactively modulate fatty acid (FA) incorporation into bacterial membranes. The triglyceride lipase facilitates elongation of incoming FAs and impacts membrane composition. Saturated and unsaturated FAs compete for entry *via* binding protein FakB1. The events dictated by prophage status illustrate how competitive processes impact membrane flexibility and bacterial fitness in lipid-rich

environments. These findings highlight the importance of assessing prophage status and lipid environments when evaluating infection risk and therapy efficiency.

Abstract

Lipids are essential components of bacterial membranes and phages are quasi-ubiquitous in bacteria. Both are crucial mediators of bacteria-host interactions. In the major pathogen *Staphylococcus aureus*, two common prophages, ϕ11.1 and ϕ13, are preferentially integrated in lipases genes: respectively encoding Geh, a triglyceride lipase, and Hlb, a sphingomyelinase. Here we discovered that ϕ11.1 and ϕ13 prophage statuses interactively determine bacterial growth, fatty acid (FA) incorporation and elongation *via* their synthesis pathway (FASII), and membrane composition. Remarkably, FASII-mediated elongation of C18:2 issued from triglycerides was stimulated by intact Geh, *i.e.*, in non-ϕ11.1 lysogens. Secondly, while *hlb* has no direct role in triglyceride metabolism, it inhibited C18:2 incorporation from di- and tri-glycerides into bacterial membrane as observed in non-ϕ13 lysogens. We show that these interactions are based on competition between Geh-generated fatty acids from tri- and di-glycerides, and Hlb-generated C16, for binding the fatty acid kinase FakB1 subunit. These findings lead to a mechanistic model in which prophage regulates the dynamics of lipid utilization, which in turn dictates FA toxicity, FASII activity and bacterial fitness. We suggest that testing new therapeutics against *S. aureus* should consider prophage status and environmental lipids for accurate prediction of efficiency.

46 **Introduction**

47 Environmental lipids comprise an integral, but often overlooked, aspect of bacterial
48 pathogenesis. Lipids are crucial for bacterial fitness and are front-line players in modulating
49 interactions with the host (1-4). Lipids range in structure from simple short hydrocarbon chains
50 to complex molecules, including triglycerides (TGs), phospholipids (PLs), sterols and their esters.
51 Fatty acids (FAs), the basic constituents of complex lipids, vary in chain length, side chains, and
52 number and position of double bonds. A vast array of bacteria scavenge FAs, which they
53 incorporate into their membranes (5-11). This quasi-ubiquity suggests a great potential of the
54 host lipid environment to modulate invading pathogen behavior. The environmental lipid
55 composition depends on human genetics and diet and is correlated to infection risk (2, 3, 12, 13).
56 *Staphylococcus* aureus, a major human pathogen, incorporates exogenous FAs, such as those
57 present in plasma lipids (6, 14). Incorporation involves a FA kinase, FakA, whose preference for
58 saturated and unsaturated FA is reportedly respectively conferred by the FA binding proteins
59 FakB1 and FakB2 (15-17). While *S. aureus* does not synthesize unsaturated and polyunsaturated
60 FAs (UFAs and PUFAs), their incorporation has documented effects on bacterial membrane
61 functions and interactions with the host (18-22).

62 Remarkably, two commonly found *S. aureus* prophages, ϕ11-1 and ϕ13, are inserted in *geh* and
63 *hlb* genes encoding lipases, respectively Geh glycerol ester hydrolase (EC 3.1.1.3) and Hlb neutral
64 sphingomyelinase C (EC 3.1.4.12) (23, 24) (Fig. 1A). About 15% of *S. aureus* isolates carry ϕ11.1
65 into *geh* and at least 90% of human clinical isolates carry ϕ13 into *hlb* (1, 25). In contrast ϕ13
66 prophage was quasi-absent in livestock isolates. ϕ11-1 and ϕ13 prophage excision is induced by
67 environmental signals (such as SOS response or biocide/H_2O_2 respectively), leading to
68 reactivation of Geh and Hlb activities with consequent impacts on *in vivo* inflammatory responses

69 (1, 26-31). In contrast consequences of lipase genes inactivation by ϕ11.1 and ϕ13 on *S. aureus*
70 metabolism and physiology have been little explored (14). Here we show that these two
71 widespread prophages interactively affect membrane phospholipid composition and growth
72 response to toxic UFA C18:2. The FA binding protein FakB1 is identified as a control point for
73 phage-dependent dynamic competition between FAs issued from triglycerides and
74 sphingomyelins.

75

76 **Results**

77 **ϕ13 lysogeny increases C18:2 incorporation from serum into *S. aureus* phospholipids.** We
78 analyzed FA profiles from two isogenic Newman strains (WT and Δϕ13), which differ by the
79 presence of ϕ13 prophage (21). The ϕ13-lysogenized WT and Δϕ13 strains showed identical FA
80 profiles in control BHI medium,, indicating that FASII-synthesis was unaffected by ϕ13 (Fig. S1).
81 In contrast, addition of 10% mouse serum to medium distinguished the two strains by their
82 incorporation of UFAs. The Δ ϕ13 strain had approximately two times less UFAs than the WT (6
83 ± 1% *versus* 13 ± 1%), including oleic acids C18:1Δ9, C18:1Δ11, and the PUFA linoleic acid C18:2
84 (Fig. 1B). Serum was the only UFA source for *S. aureus*, which lacks UFA synthesis and desaturase
85 functions (32). These results thus suggested an unexpected link between ϕ13 lysogenic status
86 and UFA incorporation from a serum source.

87 **ϕ11.1 lysogeny decreases trilinolein-derived C18:2 incorporation, elongation and toxicity; ϕ13**
88 **effects depend on ϕ11.1 status**. Trilinolein (TNL), a TG with three C18:2, is a substrate for Geh
89 lipase (33). We asked how the *geh/*ϕ11.1 status impacts breakdown of TNL to C18:2, and whether
90 ϕ13 lysogeny affects this process. For this, we analyzed FA profiles of isogenic Newman strains
91 lysogenized or not with ϕ11 (including the three ϕ11.1 to ϕ11.3 prophages) and ϕ13 prophages

92 (21). In BHI medium, the ϕ11 prophage status had no detectable effect on FA profiles which
93 reflect endogenous FA synthesis (Fig. S1). In contrast, TNL addition led to marked differences in
94 FA profiles and growth: the ϕ11 lysogenized strains showed markedly less C18:2 incorporation
95 from TNL and improved growth compared to non- ϕ11 lysogens (Fig. 1C). This result is in
96 accordance with *geh* inactivation by ϕ11.1 and C18:2 toxicity on *S. aureus* (34). The remaining
97 18:2 incorporation in the ϕ11 lysogens may indicate residual Geh activity despite the C-terminal
98 truncation, or C18:2 release by other lipases. Strikingly, ϕ11 lysogeny correlated with a quasi-
99 total inhibition of C18:2 elongation by FASII (Fig. 1C) suggesting that Geh facilitates accessibility
100 of TNL-derived C18:2 to FASII pathway. Furthermore, the ϕ13 lysogeny had effects depending on
101 the ϕ11 status. Indeed when ϕ11.1 was present, ϕ13 lysogeny led to higher C18:2 incorporation
102 from TNL (11 ± 1% in WT *versus* 4 ± 0.5% in Δϕ13 strain). In contrast, in absence of ϕ11.1 (intact
103 *geh*), it did not impact the C18:2 incorporation (28 ± 4% in Δϕ11 *versus* 28 ± 1% in Δϕ11Δϕ13
104 strain, Fig. 1C) but increases elongation of both C18:2 (from 50 to 70%) and C20:2 (from 14 to
105 28%). These observations point to an unexpected interconnection between *S. aureus* ϕ11 and
106 ϕ13 prophages for both incorporation and elongation of the PUFA C18:2 from TNL.

107 **A *geh* mutant shows decreased incorporation of trilinolein-derived C18:2 and its elongation.**
108 We asked whether ϕ11 prophage family effects were due to *geh* gene interruption by ϕ11.1. We
109 analyzed the strain USA300 which lacks ϕ11.1 (intact *geh*) and its isogenic *geh::tn* mutant. While
110 TNL-derived C18:2 was incorporated and efficiently elongated in both these strains,
111 incorporation and particularly elongation were markedly lowered in the USA300 *geh::tn* mutant
112 (Fig. 1D). Both *geh*::tn mutant and ϕ11 Newman lysogens encode C-terminal truncations of Geh
113 (at respective amino acid [aa] positions 517 and 643 from a full length protein of 690 aa).
114 Furthermore, orlistat, an inhibitor which binds to Geh (35), inhibited both incorporation and
115 elongation of C18:2 from TNL (Fig. 1D). These results indicate that the Geh state, rather than an

116 intrinsic property of ϕ11.1, determines *S. aureus* capacity to both incorporate and elongate TNL-
117 derived C18:2.

118 **1,3-diglyceride-derived C18:2 is efficiently incorporated and toxic for growth.** In TGs, the UFA
119 position on the glycerol backbone affects its absorption and metabolism by cells (36-38).
120 Triglyceride lipases display positional selectivity, which can be discriminated using 1,2-
121 dilinoleoylglycerol (1.2DG) and 1,3-dilinoleoylglycerol (1.3DG) as substrates (39-41). Geh
122 reportedly cleaves TNL in both positions 1 and 2 whereas most lipases prefer position 1 (40, 41).
123 Consequently, Geh activity liberates 1.3DG from TNL, in contrast to other lipases. We therefore
124 examined C18:2 incorporation from 1.2DG and 1.3DG in WT, Δϕ11, Δϕ13 and Δϕ11Δϕ13
125 Newman isogenic strains. Addition of 30 µM 1.2DG led to low-level C18:2 incorporation whatever
126 the prophage status. A growth retardation was observed in the Geh$^+$ strains (non-ϕ11.1 lysogens)
127 where both incorporation and elongation were favored (Fig. 1E). The same concentration of
128 1.3DG lead to lysis of non-ϕ11.1 lysogens (data not shown). Lowering 1.3DG addition to 10 µM
129 avoided lysis. Under this condition, very high incorporation and elongation of C18:2 clearly
130 occurred only when Geh is intact (in non-ϕ11.1 lysogens). TG hydrolysis product, particularly
131 attributed to Geh activity, leads therefore to high PUFA incorporation and elongation in *S. aureus*.

132 **Serum-derived C16 incorporation is increased in Δ ϕ13 and *hlb*$^+$ strains.** We focused on possible
133 mechanisms involved in ϕ13 impact on UFAs incorporation. In the presence of 10% mouse serum,
134 the percentage of C16 and its derived FAs (C18 + C20) was decreased in Newman WT strain
135 compared to the Δϕ13 strain in favor of incorporated serum UFAs (Fig. 2A). Serum
136 sphingomyelins are dominant circulating Hlb substrates that contain mainly C16 as FA moieties
137 (42, 43). To further understand how *hlb* affects UFAs utilization, we complemented the USA300
138 *hlb::tn* mutant with a plasmid carrying an intact *hlb* gene. Hlb complementation increased C16

139 and elongated derived FAs whereas it decreased incorporated serum UFAs (Fig. 2B). These results
140 indicate that *hlb* contributes to C16 liberation and its further incorporation whereas ϕ13 lysogeny
141 increases serum UFAs incorporation. Based on these observations, we hypothesized that the ϕ13
142 lysogenic/excised status likely creates a dynamic competition between C16 and UFA from serum
143 TGs for incorporation in membrane phospholipids.

144 **Incorporation of 1.3DG-derived C18:2 requires *fakB1*.** The FakA kinase preference for saturated
145 and unsaturated FA incorporation is reportedly conferred by FakB1 and FakB2, respectively (15-
146 17). We first confirmed the reported phenotypes in USA300 derivative *fakA*, *fakB1*, and *fakB2*
147 mutants in keeping with a minor role of FakB1 in UFAs incorporation, including that of free C18:2
148 PUFA (Fig. S2 and S3)(15, 17)). We then challenged USA300 derivative *fakA*, *fakB1*, and *fakB2*
149 mutants with TNL. The *fakA* mutant failed to incorporate TNL-derived C18:2 (data not shown).
150 Unexpectedly, *fakB1* and *fakB2* mutants failed to show selectivity when TNL was used as C18:2
151 precursor; both mutants displayed the capacity to incorporate C18:2 from TNL (Fig. S4). Thus,
152 while free C18:2 incorporation was FakB2-dependent (see Fig. S3), incorporation from TNL-
153 derived C18:2 was permissive. The strong effects of 1.3DG on non-ϕ11.1 lysogens growth and on
154 C18:2 incorporation, compared to 1.2DG (Fig. 2), led us to examine incorporation of these
155 substrates in *fakA*, *fakB1*, and *fakB2* backgrounds. *fakA* was essential for incorporation of both
156 substrates, reflecting the phosphorylation requirement ((15); data not shown). Incorporation of
157 1.2DG-derived C18:2 was in accordance with the reported FakB2 binding phenotype (15-17) (Fig.
158 S5). In contrast, incorporation of 1.3DG-derived C18:2 was remarkably greater in *fakB2* than in
159 *fakB1* mutant (20 ± 7% versus 13 ± 3%) and *fakB1* inactivation results in markedly lower
160 incorporation compared to the USA300 wild type (13 ± 3 % and 31 ± 5% respectively, Fig. 3A).

161 To confirm the direct role of *fakB1*, we used RN450 strain, cured of phage lysogens and with a
162 natural *fakB1* in-frame deletion (483-bp within the 867-bp functional gene, Fig. S6) and the
163 isogenic RN450-R strain, repaired for *fakB1*. The RN450-R repaired strain incorporated more
164 1.3DG-derived C18:2 than RN450 strain (35 ± 3% and 27± 3% respectively, Fig. 4A). Furthermore
165 1.3DG impairs more growth of *fakB1* defective strains (the USA300 *fakB1* mutant and RN450
166 strain) compared to their respective *fakB1*$^{+}$ controls (WT USA300 and RN450-R, Fig. 3; Fig. 4).
167 These observations identified therefore FakB1 binding as the unconventional preferred pathway
168 for efficient incorporation of 1.3DG-derived C18:2 into PL and as a contributor of growth
169 protection.

170 **1,3-diglyceride-derived C18:2 and C16 compete for FakB1.** The unexpected role of FakB1 in
171 C18:2 incorporation from tri- and di-glycerides (Fig. S4A, 3A, 4A) led us to ask whether C16,
172 favored in *hlb*$^{+}$ strains, competes for FakB1. To test this, C16 was also added in experiments
173 discussed above. We first established that, as reported, free C16 and free C18:2 were poorly
174 competitive ((17), Fig. S3). In the *fakB1* background (USA300 WT and *fakB2* mutant), addition of
175 free C16 led to a slight decrease in C18:2 incorporation from either TNL or 1.3DG (Fig. S4, Fig 3).
176 The 1.3DG-derived C18:2 incorporation is little affected in the WT (22 ± 1 % compared to 31 ±
177 5%) and unaffected in the *fakB1* mutant (14 ± 4 % compared to 13 ± 3%). In contrast, when only
178 FakB1 is available (in the *fakB2* mutant), C16 addition led to a quasi-total arrest of C18:2
179 incorporation (Fig. S4, Fig 3). As example, *fakb2* mutant has more than three times less 1.3DG-
180 derived C18:2 in the presence of C16 (6 ± 3% compared to 20 ± 7%). In RN450 (naturally fakB1
181 defective), *fakB2* can compensate for C18:2 incorporation from 1.3DG but C16 had no
182 competitive effect (Fig. 4). A direct role for *fakB1* was confirmed using RN450-R, repaired for
183 *fakB1.* Notably, total incorporation of 1.3DG-derived C18:2 is highly increased in this strain and

184 quasi-totally inhibited (80 ± 10% decreased) in the presence of free C16 (Fig. 4). FakB1 is
185 therefore a key determinant responsible for competition between C16 and 1.3DG-derived C18:2.

186

187 **Discussion**

188 *S. aureus* metabolism of environmental lipids is modulated by two common prophages, ϕ11.1
189 and ϕ13, which interrupt the lipases encoding genes *geh* and *hlb*. The present work reveals a
190 more complex role of these prophages on exogenous lipid utilization than previously supposed.
191 We identified three interactive factors that determine the bacterial responses: the
192 environmental lipids offered, which are highly variable according to the biotope; the status of
193 prophages, which toggle the lipase switches and control FAs integration in the membrane; and
194 the FA kinase FakB1, which controls competitive entry of PUFA and saturated FAs released from
195 lipids. Expanded roles for Geh, Hlb and FakB1 in *S. aureus* physiology were thus uncovered. Our
196 work demonstrates that lysogeny by ϕ11.1 and ϕ13 protects bacteria from lipid toxicity and
197 expands membrane flexibility, thus conferring a selective benefit for prophage maintenance. We
198 propose a model for two-level control of FA incorporation and elongation, first by prophages,
199 and then by FakB1 (Fig. 5).

200 The first control is determined by ϕ11.1 lysogeny, which protects *S. aureus* from PUFA toxicity.
201 When TG is available, ϕ11.1 lysogens carrying truncated Geh show decreased PUFA C18:2
202 incorporation and limited elongation. To our knowledge this is the first report of the impact of
203 Geh on FASII elongation efficiency. PUFAs provoke membrane permeabilization and lysis (44-49).
204 Unlike most lipases, Geh cleaves the TG acyl group at both positions on the glycerol backbone
205 liberating both 1,2- and 1,3-diglycerides (40, 41). Direct 1.3DG addition led to greater C18:2

206 toxicity than did 1.2DG. By inactivating Geh, ϕ11.1 lysogeny exerts a protective role on *S. aureus*
207 by limiting PUFA incorporation in membrane phospholipids, and likely improves bacterial survival
208 in natural lipid-rich environments. Considering ϕ13 lysogeny, its prevalence among human
209 clinical *S. aureus* isolates (25) suggests a functional benefit of preventing Hlb activity. As
210 expected, *hlb,* intact in the absence of ϕ13, led to increased saturated FA incorporation from
211 serum. Remarkably however, intact *hlb*, which is not implicated in PUFA metabolism, also
212 reduced PUFA incorporation and elongation.

213 FakB1 defines the second level of control. While FakB1 is reportedly associated with saturated
214 FA binding (15-17), it also mediated efficient incorporation of C18:2 issued from 1.3DG. Entry of
215 1.3DG -derived C18:2 contrasts with both free and 1.2DG-derived C18:2, which involved mainly
216 FakB2. Thus FakB1 binding is more permissive than initially reported, in accordance with recent
217 studies (15, 17, 50). FakB1 may act as a chaperone that controls free C18:2, toxic on FASII (34),
218 prior to membrane incorporation. It may also promote FakA-mediated phosphorylation of FAs,
219 which is required for C18:2 efflux *via* FarE (51). Further investigation is needed to identify the TG
220 intermediate recognized by FakB1 and Geh contribution to these binding specificities.

221 The unexpected role of FakB1 in facilitating PUFA incorporation revealed a newly identified role
222 of *hlb* in an interference with unsaturated FAs incorporation. Hlb activity in ϕ13 non-lysogens
223 increases entry of saturated FAs, which bind FakB1, and compete with PUFA. FakB1 is a
224 gatekeeper that discriminates between PUFA and saturated FA incorporation in membrane
225 phospholipids. If PUFA-FakB1 binding is out-competed by saturated FAs, *S. aureus* survival could
226 be compromised due to deficient FakB1 and FarE protecting effects. We propose that the
227 combined effects of prophages and FakB1 on FA incorporation are relevant to *S. aureus* infection.
228 Both ϕ11.1 and ϕ13 phage may be maintained episomally and reintegrated, implying transient

229 activation of *geh* and *hlb* expression; these events may help adjust bacterial membrane lipids
230 during infection (25-30, 52). PUFAs may in turn impact the life cycle of these prophages.

231 The composition and levels of TGs and SMs vary among individuals and according to dietary
232 intake. These factors are determinants of infection risk and predisposition to bacterial resistance
233 (43, 53-57). TGs are major reservoirs of long chain UFAs and PUFAs liberated by Geh activity and
234 incorporation of these FAs alters bacterial membrane functions and host interactions (6, 18, 19,
235 22, 58). Cholesterol was recently reported to be a Geh substrate (18); its effects on *S. aureus*
236 fitness according to prophage status remains to be investigated. Interestingly, intact Geh
237 contributes to masking *S. aureus* from the immune surveillance by TLR2 receptor (1, 59) and 1,2-
238 diglycerols moieties are involved in the interaction TLR2 (60). Roles of position 2 hydrolysis and
239 ϕ11.1 lysogeny in immune escape merit further investigation.

240 The *in vivo* significance of ϕ13 impacts on PUFAs incorporation and elongation is intriguing.
241 Specific interference by Hlb in PUFA incorporation is an interesting new avenue to investigate
242 ϕ13 maintenance in the *hlb* locus specifically in healthy human host (25,61). Indeed
243 sphingomyelins and their metabolites vary between animals and in disease associated to atypical
244 ϕ13 integration (62, 63).

245 In conclusion, ϕ11.1 and ϕ13 are interactive regulators of *S. aureus* membrane phospholipid
246 composition in response to environmental TGs and SMs. Our findings lead us to suggest that
247 prophage lysogeny contributes to protecting bacteria from lipid toxicity. Prophage instability also
248 offers greater membrane flexibility, which contribute to *S. aureus* adaptation in different host
249 biotopes. In particular, while Hlb (ß toxin) is required for *S. aureus* virulence in humans, we
250 showed that the associated production of C16 results in an increase of free 1.3DG-derived C18:2
251 that is toxic for bacteria. Thus, by controlling the cytoplasmic availability of C18:2 and C16,

252 respectively, ϕ11.1 and ϕ13 exert a fine tuning between metabolism and toxicity. These results
253 provide new mechanistic insights of *S. aureus* lipid physiology and indicate the need to assess
254 mechanisms of prophage/lipase switches in developing strategies against *S. aureus* infection.

255

256 **Materials and methods**

257 **Bacterial strains.** *S. aureus* Newman, USA300 FPR3757 JE2 (called here USA300), and NCTC 8325
258 derivative strains RN450 and RN450-R, were used in this study. Isogenic Newman strains
259 differentiated by the presence of prophages were provided by Dr O. Schneewind (Department of
260 Microbiology, University of Chicago). Newman strain has 4 prophages which are from
261 Siphoviridae family: ϕ11.1, ϕ11.2 and ϕ11.3 from Sfi 11/Sa6 subfamily and ϕ13 from Sfi 21/Sa3
262 subfamily (24). Methicillin-resistant USA300 and the Nebraska library of transposon insertions
263 (University of Nebraska Medical Center) were generously supplied by BEI resources (64). USA300
264 derivatives from this library used in this work contained insertions in the following genes:
265 SAUSA300_0320 (*geh*), SAUSA300_1973 (*hlb*), SAUSA300_1119 (*fakA*), SAUSA300_0733 (*fakB1*),
266 SAUSA300_1318 (*fakB2*); all mutants were verified by PCR. RN450 is a phage-free derivative of
267 the NCTC 8325 strain (65). It was repaired for a natural *fakB1* deletion as described for another
268 strain (66).

269 **Construction of *hlb* complemented strain.** A PCR fragment containing the *S. aureus* subsp.
270 *aureus* COL *hlb* promoter and open reading frame from SACOL_RS10470 (-355 from ATG start
271 codon and +40 after TAG stop codon) was cloned in EcoRI and SmaI sites of modified pAW8 (67).
272 The primers pairs used for the PCR are 5'-TTGCCGGAATTCTGCAACTTAATTATAGCCAGACTTTC-3'
273 and 5'-CATCAACCCGGGCGTCCTTTTAGAACGAAGCAAG-3'. Genomic co-ordinates of the 1388 bp
274 cloned segment are 2063371-2064758, as present on plasmid phlb.

275 **Construction of *fakB1*-repaired strain.** The *fakB1* gene of *S. aureus* RN450, as the entire NCTC
276 8325 lineage, displays a 483-bp deletion removing 56% of the 867-bp functional gene (Fig. S6).
277 To repair this deletion, a 1,939-bp DNA fragment containing a functional *fakB1* was amplified as
278 described for other NCTC 8325 derivatives (66). The *fakB1*-repaired strain is designated as
279 RN450-R.

280 **Growth media.** Brain heart infusion (BHI) was the base medium for *S. aureus* cultures unless
281 specified. Cultures were grown aerobically at 37°C and the starting OD_{600nm} was 0.02 from a
282 preculture at OD_{600nm} between 1 and 5. Mouse serum (Clinisciences, France) was added at 10%
283 final concentration. Stocks of trilinolein (TNL, 50 mM), 1,2-dilinoleoylglycerol (1.2DG, 50 mM),
284 1,3-dilinoleoylglycerol (1.3DG, 50 mM), palmitic acid (C16, 100 mM) (Larodan Fine Chemicals,
285 Sweden) and orlistat (38 mM, MedChemExpress) were prepared in DMSO.

286 **Determination of *S. aureus* fatty acid profiles.** FA profiles were performed as described (7). For
287 each condition, profiles were determined from three independent cultures. In these experiments
288 culture aliquots were routinely taken under exponential growth at OD_{600} between 0.5 and 2.
289 After sample preparation (7), analyses were performed in a split-splitless injection mode on an
290 AutoSystem XL Gas Chromatograph (Perkin-Elmer) equipped with a ZB-Wax capillary column (30
291 m x 0.25 mm x 0.25 mm; Phenomenex, France). Data were recorded and analyzed by TotalChrom
292 Workstation (Perkin-Elmer). FA peaks were detected between 12 and 40 min of elution, and
293 identified by comparing to retention times of purified esterified FA standards (Mixture ME100,
294 Larodan, Sweden). Results are shown as representative gas chromatograph profiles, or as percent
295 of specific FAs as calculated from their proportions compared to total peak areas (TotalChrom
296 Workstation; Perkin Elmer).

297 **Statistics analysis.** Graphs were prepared using Microsoft Excel software. Means and standard
298 deviations are presented for culture growth (OD_{600nm}/h) and FA percentages. Statistical
299 significance was determined by unpaired, nonparametric Mann Whitney tests (U test calculator,
300 Wilcoxon rank-sum, https://www.statskingdom.com), as recommended for small sample sizes.

301 **Acknowledments:** We gratefully acknowledge funding from the following French granting
302 agencies: French Agence Nationale de la Recherche (StaphEscape project ANR-16-CE15-0013),
303 and the Fondation pour la Recherche Medicale (DBF20161136769). We thank Myriam Gominet
304 for the construction of *S. aureus* RN450 *fakB1*-repaired strain.

305

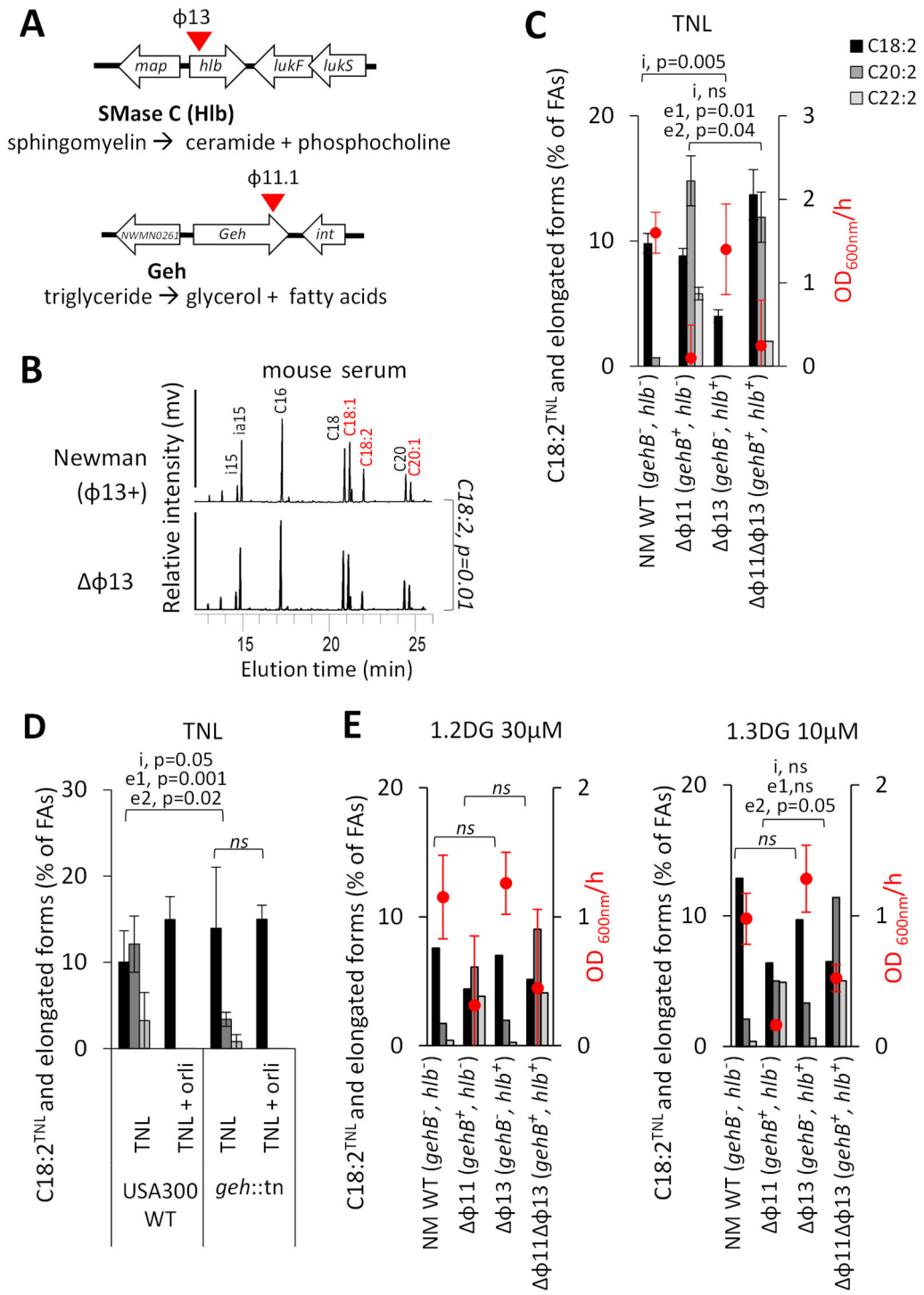

FIG 1 *S. aureus* lysogenic status impacts incorporation and elongation of C18:2 derived from acylglycerides.

(*A*) Upper, site of ϕ13 insertion in *hlb*, encoding sphingomyelinase (Hlb). ϕ13 insertion results in enzyme N-terminal truncation (position 56 aa of the 330 aa protein). Lower, preferred site of ϕ11.1 insertion is *geh*, encoding triacylglycerol lipase (Geh). ϕ11-1 insertion results in truncation of the encoded triglyceride Geh (position 643 aa of the 690 aa protein).

(*B*) ϕ13 lysogen displays greater C18:2 incorporation from mouse serum than non-lysogen. The Newman strain (wild type, WT), a ϕ13 lysogen, and an isogenic Δϕ13 derivative were grown 2h in BHI medium containing 10% mouse serum. FAs were extracted and analyzed by gas

316 chromatography. The y axis represents relative FA abundance (mV response) at indicated peak
317 positions. Black arrows indicate FAs that can be endogenously produced. Red arrows indicate FAs
318 not synthesized by *S. aureus* but incorporated from serum. Representative FA profiles from four
319 determinations are shown.
320 (*C*) ϕ13 and ϕ11 prophages interfere to modulate C18:2 incorporation and elongation from
321 trilinolein. Four isogenic Newman strains (NM) vary in prophage content, including ϕ11.1 and
322 ϕ13 (21). These isogenic strains were grown 2h in BHI medium supplemented with 30µM
323 trilinolein (comprising 3 oleic acid moieties). Growth is presented as the absorbance increase in
324 one hour (OD_{600nm}/h). Proportions of C18:2 and elongated forms (C20:2 and C22:2) were
325 determined from the FA profiles as in (*A*) and presented as percent of the total FA areas for each
326 profile (n=5).
327 (*D*) *geh* truncation decreases both incorporation and elongation of C18:2 from trilinolein. C18:2
328 incorporation from trilinolein is favored when *geh* is intact. USA300 (*geh*$^+$) and the *geh*::tn, were
329 grown in media supplemented with TNL. The Geh inhibitor orlistat (orli; 30 µM) was added as
330 indicated. The confirmed *geh*::tn mutant has a C-terminal truncated Geh (position 517 aa/690aa).
331 The percent of C18:2 and its elongated forms were determined as in (B). The OD/h of the *geh*::tn
332 mutant and the wild type were comparable (0.8 ± 0.3 for both cultures), (n=3).
333 (*E*) Acylated positions in a diglyceride determine C18:2 incorporation into *S. aureus* membrane
334 phospholipids**.** The four isogenic Newman strains, which differ in ϕ11.1 and ϕ13 prophages (21)
335 were grown 2h in BHI medium supplemented with 30 µM diglycerides comprising linoleic acid
336 moieties; 1,2-dilinoleoylglycerol (1.2DG) or 10µM 1,3-dilinoleoylglycerol (1.3DG), (n=4). Note
337 that 1.3DG was more incorporated and more toxic than 1.2DG; 30µM 1.3DG generated cell lysis
338 and FA profiles of unrepresentative non-lysed subpopulation (not shown). Studies were
339 therefore with 10µM. Percent of C18:2 and its elongated forms were determined as in (*B*). FA
340 profiles and percent of C18:2 and elongated forms are described as in (*B*).
341 p-values were determined by Mann Whitney test on percent total incorporated C18:2, including
342 elongated forms ('i'), and on percent elongation of C18:2 ('e1'), and C20:2 ('e2'); n.s., not
343 significant.
344

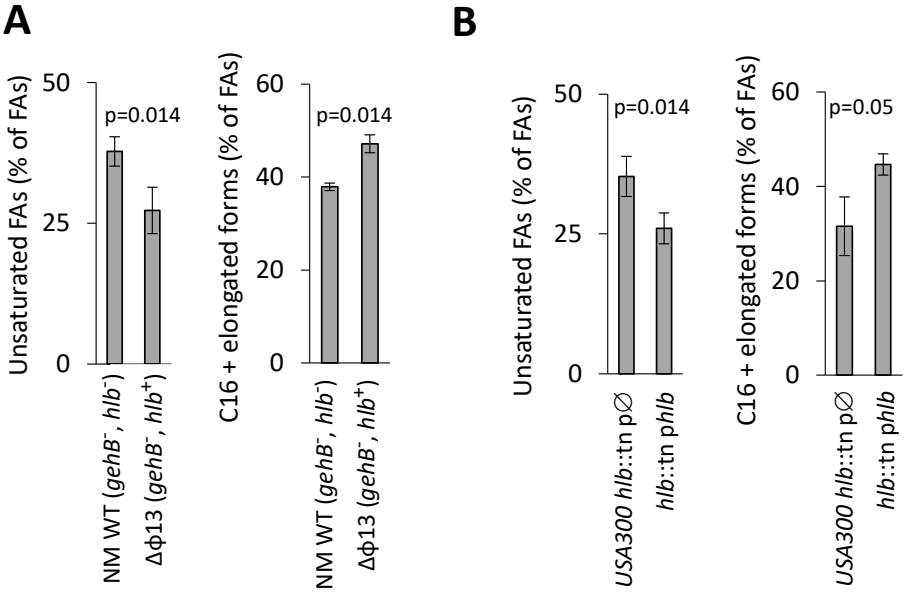

FIG 2 Intact *hlb* favors incorporation of saturated FAs and decreases incorporation of UFAs from serum. (*A*) Newman (NM) WT and Δϕ13 cultures were grown for 2 hours in BHI medium supplemented with 10% mouse serum. The proportion of UFAs (left) and SFAs (right) are shown. ϕ13 lysogeny increases unsaturated FAs while lowering incorporation of C16 and elongated forms. (*B*) Plasmid-driven expression of *hlb* increases incorporation of C16 and elongated forms, while lowering incorporation of unsaturated FAs. Cultures of the USA300 (USA) *hlb*::tn p∅ strain bearing an empty plasmid or a plasmid carrying intact *hlb* (pHlb, derived from the COL strain) were grown for 2.5 h in BHI supplemented with 10% mouse serum. FA extractions were performed and FA profiles and area of FAs were determined as in Fig. 1. Proportions of saturated FAs (C16, C18and C20) and unsaturated FAs (C18:1Δ9, C18:1Δ11, C18:2 and C20:1) were compared to total FAs (shown as percent of total). Data presented are means ± standard deviations from three independent experiments. p-values were determined by Mann Whitney test.

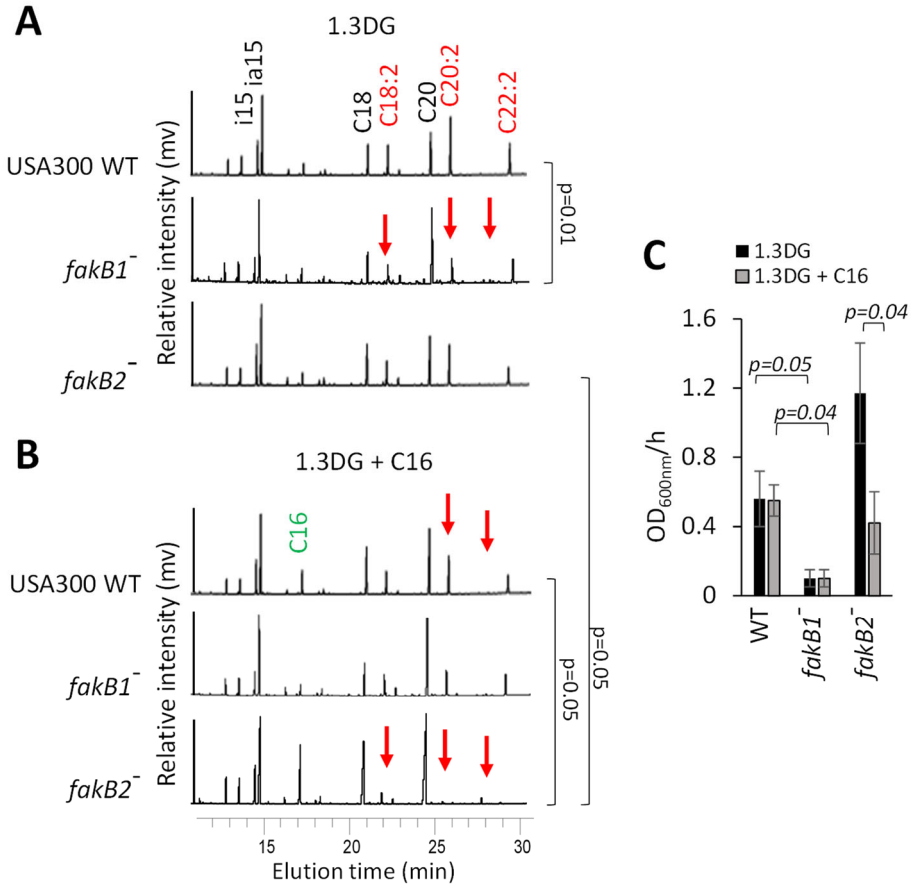

FIG 3 *fakB1* and C16 modulate 1.3DG-derived C18:2 incorporation and its toxicity on growth. (*A*) Involvement of *S. aureus fakB1* in 1.3DG-mediated C18:2 incorporation. USA300, *fakB1* and *fakB2* strains were grown 2 hours in BHI supplemented with 10µM 1.3DG. (*B*) 1.3DG-derived C18:2 and C16 compete for FakB1. Effects of C16 (20 µM) addition on C18:2 incorporation from 1.3DG were assessed in USA300, *fakB1*, and *fakB2* strains, as in (*A*). Representative FA profiles are shown in (A) and (B), (n=5). (*C*) Growth of WT and *fakB* mutants under conditions described in (*A*) and (*B*), presented as OD_{600nm} per hour. Representative profiles (*A*, *B*) or means (*C*) from four independent experiments are presented. p-values were determined by Mann Whitney test for percent incorporated C18:2, including elongated forms and OD/h.

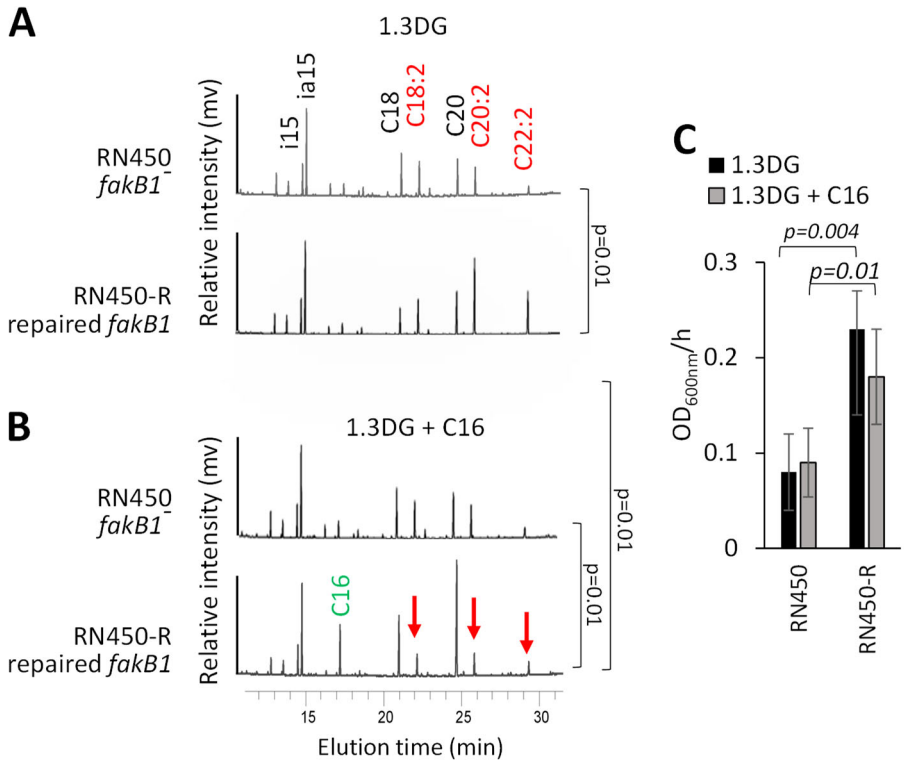

FIG 4 Competition between 1.3DG-derived C18:2 and C16 at *fakb1* shapes incorporation into phospholipid. (*A*) FA profiles of RN450 (*fakB1*$^-$) and RN450-R (*fakB1*$^+$) grown 2.5 h in BHI supplemented with 10µM 1.3DG without or with 40µM C16. (*B*) Growth of RN450 and RN450-R cultures from (*A*). Data presented are representative profiles (A) or means (C) from five independent experiments. p-values were determined by the Mann Whitney test for percent incorporated C18:2 (including elongated forms (*A*) and OD/h (*B*).

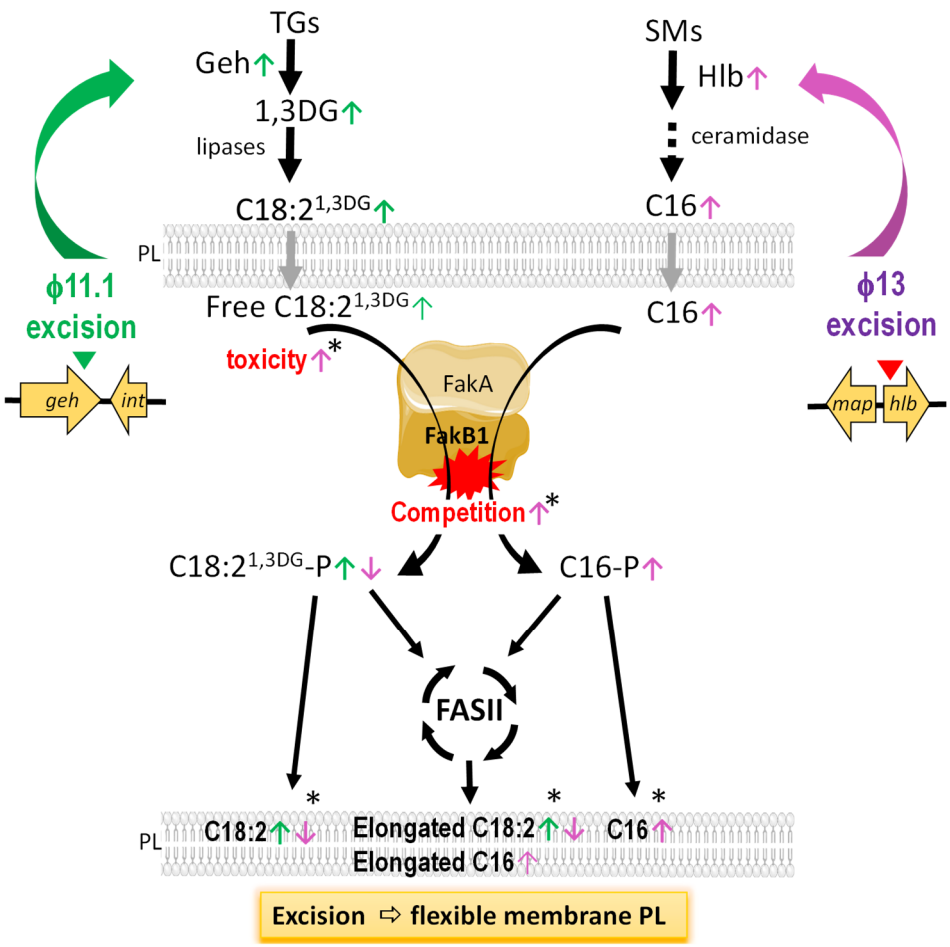

FIG 5 A mechanistic model for environmental lipid utilization by *S. aureus*; ϕ11.1, ϕ13 and *fakB1* are lipid toxicity and membrane flexibility checkpoints.

ϕ11.1 lysogeny protects *S. aureus* from toxic C18:2 incorporation from triglyceride. ϕ11.1 in *geh* prevents TG hydrolysis, so that *S. aureus* incorporates low amounts of C18:2. In the absence of ϕ11.1, or upon stress-induced excision, intact Geh allows TG hydrolysis to 1.3 DG which promotes C18:2 incorporation. 1.3DG-derived C18:2 ($C18:2^{1.3DG}$) is incorporated via the FakA-FakB kinase system and the phosphorylated product ($C18:2^{1.3DG}$-P) may then be incorporated in phospholipids or cycled towards FASII for rounds of elongation before incorporation. The latter pathway is favored by intact Geh by an unknown mechanism.

FakB1 binds $C18:2^{1.3DG}$ and protects from its toxicity. Exogenous FAs are phosphorylated *via* FakAB system comprising FakA kinase and FakB1 or FakB2 acyl binding proteins, initially reported as being specialized in saturated and unsaturated FAs respectively (15, 16). Despite this bias, we showed in this study that C18:2 from TG or 1.3DG interacts with FakB1 binding protein.

Intact *hlb* interferes with binding of $C18:2^{1.3DG}$ to FakB1, with consequences on toxicity. The absence of ϕ13 (or oxidative stress condition) enables Hlb activity and liberation of C16 from serum SMs. This C16 competes with $C18:2^{1.3DG}$ for FakB1 binding and increases pools of free C18:2, which may be toxic. In contrast, ϕ13 lysogeny inactivates *hlb* and prevent sphingomyelins (SMs) hydrolysis, thus reducing competition. The entry of $C18:2^{1.3DG}$ via FakB1 may prevent intracellular toxicity and lead to FA elongation via FASII. ϕ13 lysogeny thus fine-tunes membrane flexibility via both $C18:2^{1.3DG}$ incorporation and elongation.

$C18:2^{1.3DG}$ represents C18:2 issued from 1.3DG. Impact of ϕ11.1, green arrows; impact of ϕ13, purple arrows; unknown mechanism of fatty acid diffusion, gray arrows. Experimental results of this study are indicated by the star (*).

434 **Supplementary information titles and legends**

435 **Supplementary FIG S1** ϕ11.1 or ϕ13 lysogeny has no effect on fatty acid (FA) profiles of *S. aureus*
436 grown in BHI medium. Four isogenic Newman strains, lysogenized or not by ϕ11.1 and ϕ13
437 prophages (1) were grown in BHI medium. FA were extracted at OD_{600} = 1 and analyzed by gas
438 chromatography as described in material and methods. Representative FA profiles from three
439 determinations are shown.
440
441 **Supplementary FIG S2** Validation of free fatty acids (FAs) incorporation in USA300 (WT), and
442 *fakA, fakB1* and *fakB2* mutant derivatives. The indicated strains were grown in BHI in the
443 presence of 0.17 mM each free FAs, C14:0, C16:0, and C18:1. FAs were extracted and analyzed
444 as in Fig. S1. The three exogenous FAs and elongated forms are indicated in red. Data presented
445 are representative profiles from three independent experiments.
446
447 **Supplementary FIG S3** Incorporation of free C18:2 in the *fakB2* mutant without and with C16
448 supplementation. The *fakB2* mutant was grown in BHI in the presence 10µM free C18:2 without
449 or with 40 µM C16, and fatty acids (FAs) were extracted and analyzed as in Fig. S1. C16 in upper
450 panel corresponds to endogenous synthesis; the higher C16 peak in lower panel reflects
451 exogenous FA addition. Exogenous FAs or their elongated forms are represented in red. Data
452 presented are representative profiles from three independent experiments.
453
454 **Supplementary FIG S4** *fakB1* and *fakB2* mutants both mediate C18:2 incorporation from
455 trilinolein, but only the *fakB2* mutant is affected by C16 addition. (*A*) C18:2 incorporation from
456 trilinolein in USA300 wild type and *fakB* mutants. Strains were grown two hours in BHI
457 supplemented with 30µM trilinolein, and fatty acid (FA) profiles were determined as in Fig. S1.
458 The y-axis represents relative fatty acid (FA) abundance (mV response). Exogenous FA
459 incorporated products (C18:2, C20:2, and C22:2) are in red. (B) Cultures were prepared as in (A),
460 except that 20 µM C16 was further added to medium. The *fakB2* mutant, which expresses FakB1,
461 is totally inhibited for C18:2 incorporation. Green and red arrows indicate changes due to C16
462 addition on peaks of C16, and C18:2 + elongated products, respectively. (C) Growth of WT, *fakB1*
463 and *fakB2* strains in the presence of trilinolein supplemented or not with C16. Samples
464 correspond to those presented in (*A*) and (*B*); results are presented as OD_{600nm} per hour. Data
465 are representative profiles, (*A* and *B*) or means (*C*) from three independent experiments.
466
467 **Supplementary FIG S5** *fakB2*, and not *fakB1*, affects C18:2 incorporation from 1,2-
468 dilinoleoylglycerol (1.2DG). C18:2 incorporation from 1.2DG was assessed in USA300 WT, *fakB1*,
469 and *fakB2* strains. Strains were grown two hours in BHI supplemented with 30µM 1.2DG, and
470 fatty acids (FA) profiles were determined as in Fig. S1). Exogenous FA incorporated products
471 (C18:2, C20:2, and C22:2) are in red. The *fakB2* mutant shows significant inhibition of the
472 cumulative percentage of C18:2 and elongated forms (10 ± 3 %) compared to wild type (34 ± 5%).
473 Data are representative profiles from three independent experiments.
474
475 **Supplementary FIG S6** FakB1 defect in NCTC 8325 lineage, comprising RN450. Alignment of
476 FakB1 sequences from Newman (non-NCTC 8325 lineage) and NCTC 8325 strains. The non-
477 deleted region of NCTC 8325 FakB1 shares 99% identity with the synonymous region in
478 Newman. Red arrows indicate amino acids required for FA binding and for FakA-mediated
479 phosphotransfer (1).
480

481 **References**

482 1. Chen X, Alonzo F, 3rd. 2019. Bacterial lipolysis of immune-activating ligands promotes evasion
483 of innate defenses. Proc Natl Acad Sci USA 116:3764-3773.

484 2. Sun H, Zhang X, Shi W, Fang B. 2019. Association of soft tissue infection in the extremity with
485 glucose and lipid metabolism and inflammatory factors. Exp Ther Med 17:2535-2540.

486 3. Trinder M, Boyd JH, Brunham LR. 2019. Molecular regulation of plasma lipid levels during
487 systemic inflammation and sepsis. Curr Opin Lipidol 30:108-116.

488 4. Gajenthra Kumar N, Contaifer D, Jr., Baker PR, Ekroos K, Jefferson KK, Wijesinghe DS. 2018.
489 Untargeted lipidomic analysis to broadly characterize the effects of pathogenic and non-
490 pathogenic staphylococci on mammalian lipids. PLoS One 13:e0206606.

491 5. Gloux K, Guillemet M, Soler C, Morvan C, Halpern D, Pourcel C, Vu Thien H, Lamberet G, Gruss
492 A. 2017. Clinical relevance of type II fatty acid synthesis bypass in *Staphylococcus aureus*.
493 Antimicrob Agents Chemother 61: e02515-16.

494 6. Kenanian G, Morvan C, Weckel A, Pathania A, Anba-Mondoloni J, Halpern D, Gaillard M,
495 Solgadi A, Dupont L, Henry C, Poyart C, Fouet A, Lamberet G, Gloux K, Gruss A. 2019.
496 Permissive fatty fcid Incorporation promotes staphylococcal adaptation to FASII antibiotics
497 in host environments. Cell Rep 29:3974-3982.

498 7. Morvan C, Halpern D, Kenanian G, Hays C, Anba-Mondoloni J, Brinster S, Kennedy S, Trieu-
499 Cuot P, Poyart C, Lamberet G, Gloux K, Gruss A. 2016. Environmental fatty acids enable
500 emergence of infectious *Staphylococcus aureus* resistant to FASII-targeted antimicrobials.
501 Nat Commun 7:12944.

502 8. Morvan C, Halpern D, Kenanian G, Pathania A, Anba-Mondoloni J, Lamberet G, Gruss A, Gloux
503 K. 2017. The *Staphylococcus aureus* FASII bypass escape route from FASII inhibitors.
504 Biochimie 141:40-46.

505 9. Brinster S, Lamberet G, Staels B, Trieu-Cuot P, Gruss A, Poyart C. 2009. Type II fatty acid
506 synthesis is not a suitable antibiotic target for Gram-positive pathogens. Nature 458:83-6.

507 10. Brinster S, Lamberet G, Staels B, Trieu-Cuot P, Gruss A, Poyart C. 2010. Essentiality of FASII
508 pathway for *Staphylococcus aureus*. Reply. Nature 463:E4-E5.

509 11. Hays C, Lambert C, Brinster S, Lamberet G, du Merle L, Gloux K, Gruss A, Poyart C, Fouet A.
510 2021. Type II fatty acid synthesis pathway and cyclopropane ring formation are dispensable
511 during *Enterococcus faecalis* systemic infection. J Bacteriol 203:e0022121.

512 12. Feingold KR, Grunfeld C. 2000. The effect of inflammation and infection on lipids and
513 lipoproteins. *In* Feingold KR, Anawalt B, Boyce A, Chrousos G, Dungan K, Grossman A,
514 Hershman JM, Kaltsas G, Koch C, Kopp P, Korbonits M, McLachlan R, Morley JE, New M,
515 Perreault L, Purnell J, Rebar R, Singer F, Trence DL, Vinik A, Wilson DP (ed), Endotext, South
516 Dartmouth (MA). https://pubmed.ncbi.nlm.nih.gov/26561701.

517 13. Kaysen GA, Ye X, Raimann JG, Wang Y, Topping A, Usvyat LA, Stuard S, Canaud B, van der
518 Sande FM, Kooman JP, Kotanko P, Monitoring Dialysis Outcomes I. 2018. Lipid levels are
519 inversely associated with infectious and all-cause mortality: international MONDO study
520 results. J Lipid Res 59:1519-1528.

521 14. Delekta PC, Shook JC, Lydic TA, Mulks MH, Hammer ND. 2018. *Staphylococcus aureus* utilizes
522 host-derived lipoprotein particles as sources of fatty acids. J Bacteriol 200:e00728-17.

523 15. Parsons JB, Broussard TC, Bose JL, Rosch JW, Jackson P, Subramanian C, Rock CO. 2014.
524 Identification of a two-component fatty acid kinase responsible for host fatty acid
525 incorporation by *Staphylococcus aureus*. Proc Natl Acad Sci U S A 111:10532-7.

526 16. Broussard TC, Miller DJ, Jackson P, Nourse A, White SW, Rock CO. 2016. Biochemical roles
527 for conserved residues in the bacterial fatty acid-binding protein family. J Biol Chem
528 291:6292-303.

529 17. Cuypers MG, Subramanian C, Gullett JM, Frank MW, White SW, Rock CO. 2019. Acyl-chain
530 selectivity and physiological roles of *Staphylococcus aureus* fatty acid-binding proteins. J Biol
531 Chem 294:38-49.

532 18. Hines KM, Alvarado G, Chen X, Gatto C, Pokorny A, Alonzo F, 3rd, Wilkinson BJ, Xu L. 2020.
533 Lipidomic and ultrastructural characterization of the cell envelope of *Staphylococcus aureus*
534 grown in the presence of human serum. mSphere 5:e00339-20.

535 19. Nguyen MT, Hanzelmann D, Hartner T, Peschel A, Gotz F. 2016. Skin-specific unsaturated
536 fatty acids boost the *Staphylococcus aureus* innate immune response. Infect Immun 84:205-
537 15.

538 20. Bosch M, Sanchez-Alvarez M, Fajardo A, Kapetanovic R, Steiner B, Dutra F, Moreira L, Lopez
539 JA, Campo R, Mari M, Morales-Paytuvi F, Tort O, Gubern A, Templin RM, Curson JEB, Martel
540 N, Catala C, Lozano F, Tebar F, Enrich C, Vazquez J, Del Pozo MA, Sweet MJ, Bozza PT, Gross
541 SP, Parton RG, Pol A. 2020. Mammalian lipid droplets are innate immune hubs integrating
542 cell metabolism and host defense. Science 370:eaay8085.

543 21. Bae T, Baba T, Hiramatsu K, Schneewind O. 2006. Prophages of *Staphylococcus aureus*
544 Newman and their contribution to virulence. Mol Microbiol 62:1035-47.

545 22. Arsic B, Zhu Y, Heinrichs DE, McGavin MJ. 2012. Induction of the staphylococcal proteolytic
546 cascade by antimicrobial fatty acids in community acquired methicillin resistant
547 *Staphylococcus aureus*. PLoS One 7:e45952.

548 23. Lee CY, Iandolo JJ. 1985. Mechanism of bacteriophage conversion of lipase activity in
549 *Staphylococcus aureus*. J Bacteriol 164:288-93.

550 24. Goerke C, Pantucek R, Holtfreter S, Schulte B, Zink M, Grumann D, Broker BM, Doskar J, Wolz
551 C. 2009. Diversity of prophages in dominant *Staphylococcus aureus* clonal lineages. J
552 Bacteriol 191:3462-8.

553 25. Goerke C, Koller J, Wolz C. 2006. Ciprofloxacin and trimethoprim cause phage induction and
554 virulence modulation in *Staphylococcus aureus*. Antimicrob Agents Chemother 50:171-7.

555 26. Tran PM, Feiss M, Kinney KJ, Salgado-Pabon W. 2019. phiSa3mw prophage as a molecular
556 regulatory switch of *Staphylococcus aureus* beta-toxin production. J Bacteriol 201:e00766-
557 18.

558 27. Ubeda C, Maiques E, Knecht E, Lasa I, Novick RP, Penades JR. 2005. Antibiotic-induced SOS
559 response promotes horizontal dissemination of pathogenicity island-encoded virulence
560 factors in staphylococci. Mol Microbiol 56:836-44.

561 28. Tang Y, Nielsen LN, Hvitved A, Haaber JK, Wirtz C, Andersen PS, Larsen J, Wolz C, Ingmer H.
562 2017. Commercial Biocides Induce Transfer of Prophage Phi13 from Human Strains of
563 *Staphylococcus aureus* to Livestock CC398. Front Microbiol 8:2418.

564 29. Salgado-Pabon W, Herrera A, Vu BG, Stach CS, Merriman JA, Spaulding AR, Schlievert PM.
565 2014. *Staphylococcus aureus* beta-toxin production is common in strains with the beta-toxin
566 gene inactivated by bacteriophage. J Infect Dis 210:784-92.

567 30. Goerke C, Wirtz C, Fluckiger U, Wolz C. 2006. Extensive phage dynamics in Staphylococcus
568 aureus contributes to adaptation to the human host during infection. Mol Microbiol
569 61:1673-85.

570 31. Jung P, Abdelbary MM, Kraushaar B, Fetsch A, Geisel J, Herrmann M, Witte W, Cuny C,
571 Bischoff M. 2017. Impact of bacteriophage Saint3 carriage on the immune evasion capacity
572 and hemolytic potential of *Staphylococcus aureus* CC398. Vet Microbiol 200:46-51.

573 32. Parsons JB, Frank MW, Jackson P, Subramanian C, Rock CO. 2014. Incorporation of
574 extracellular fatty acids by a fatty acid kinase-dependent pathway in *Staphylococcus aureus*.
575 Mol Microbiol 92:234-45.

576 33. Cadieux B, Vijayakumaran V, Bernards MA, McGavin MJ, Heinrichs DE. 2014. Role of lipase
577 from community-associated methicillin-resistant *Staphylococcus aureus* strain USA300 in
578 hydrolyzing triglycerides into growth-inhibitory free fatty acids. J Bacteriol 196:4044-56.

579 34. Zheng CJ, Yoo JS, Lee TG, Cho HY, Kim YH, Kim WG. 2005. Fatty acid synthesis is a target for
580 antibacterial activity of unsaturated fatty acids. FEBS Lett 579:5157-62.

581 35. Kitadokoro K, Tanaka M, Hikima T, Okuno Y, Yamamoto M, Kamitani S. 2020. Crystal
582 structure of pathogenic *Staphylococcus aureus* lipase complex with the anti-obesity drug
583 orlistat. Sci Rep 10:5469.

584 36. Yoshinaga K, Sasaki K, Watanabe H, Nagao K, Inoue N, Shirouchi B, Yanagita T, Nagai T,
585 Mizobe H, Kojima K, Beppu F, Gotoh N. 2015. Differential effects of triacylglycerol positional
586 isomers containing n-3 series highly unsaturated fatty acids on lipid metabolism in C57BL/6J
587 mice. J Nutr Biochem 26:57-63.

588 37. Ikeda I, Yoshida H, Tomooka M, Yosef A, Imaizumi K, Tsuji H, Seto A. 1998. Effects of long-
589 term feeding of marine oils with different positional distribution of eicosapentaenoic and
590 docosahexaenoic acids on lipid metabolism, eicosanoid production, and platelet aggregation
591 in hypercholesterolemic rats. Lipids 33:897-904.

592 38. Schuhmacher M, Grasskamp AT, Barahtjan P, Wagner N, Lombardot B, Schuhmacher JS, Sala
593 P, Lohmann A, Henry I, Shevchenko A, Coskun U, Walter AM, Nadler A. 2020. Live-cell lipid
594 biochemistry reveals a role of diacylglycerol side-chain composition for cellular lipid
595 dynamics and protein affinities. Proc Natl Acad Sci U S A 117:7729-7738.

596 39. Lyberg AM, Adlercreutz P. 2008. Lipase specificity towards eicosapentaenoic acid and
597 docosahexaenoic acid depends on substrate structure. Biochim Biophys Acta 1784:343-50.

598 40. Douchet I, De Haas G, Verger R. 2003. Lipase regio- and stereoselectivities toward three
599 enantiomeric pairs of didecanoyl-deoxyamino-O methyl glycerol: a kinetic study by the
600 monomolecular film technique. Chirality 15:220-6. 10.

601 41. Horchani H, Ben Salem N, Chaari A, Sayari A, Gargouri Y, Verger R. 2010. Staphylococcal
602 lipases stereoselectively hydrolyse the sn-2 position of monomolecular films of diglyceride
603 analogs. Application to sn-2 hydrolysis of triolein. J Colloid Interface Sci 347:301-8.

604 42. Hammad SM, Pierce JS, Soodavar F, Smith KJ, Al Gadban MM, Rembiesa B, Klein RL, Hannun
605 YA, Bielawski J, Bielawska A. 2010. Blood sphingolipidomics in healthy humans: impact of
606 sample collection methodology. J Lipid Res 51:3074-87.

607 43. Hanamatsu H, Ohnishi S, Sakai S, Yuyama K, Mitsutake S, Takeda H, Hashino S, Igarashi Y.
608 2014. Altered levels of serum sphingomyelin and ceramide containing distinct acyl chains in
609 young obese adults. Nutr Diabetes 4:e141.

610 44. Zhang Q, Wu W, Zhang J, Xia X. 2020. Antimicrobial lipids in nano-carriers for antibacterial
611 delivery. J Drug Target 28:271-281.

612 45. Butcher GW, King G, Dyke KG. 1976. Sensitivity of *Staphylococcus aureus* to unsaturated fatty
613 acids. J Gen Microbiol 94:290-6.

614 46. Knapp HR, Melly MA. 1986. Bactericidal effects of polyunsaturated fatty acids. J Infect Dis
615 154:84-94.

616 47. Kelsey JA, Bayles KW, Shafii B, McGuire MA. 2006. Fatty acids and monoacylglycerols inhibit
617 growth of *Staphylococcus aureus*. Lipids 41:951-61.

618 48. Kabara JJ, Swieczkowski DM, Conley AJ, Truant JP. 1972. Fatty acids and derivatives as
619 antimicrobial agents. Antimicrob Agents Chemother 2:23-8.

620 49. Desbois AP, Smith VJ. 2010. Antibacterial free fatty acids: activities, mechanisms of action
621 and biotechnological potential. Appl Microbiol Biotechnol 85:1629-42.

622 50. Krute CN, Ridder MJ, Seawell NA, Bose JL. 2019. Inactivation of the exogenous fatty acid
623 utilization pathway leads to increased resistance to unsaturated fatty acids in *Staphylococcus*
624 *aureus*. Microbiology 165:197-207.

625 51. Alnaseri H, Kuiack RC, Ferguson KA, Schneider JET, Heinrichs DE, McGavin MJ. 2019. DNA
626 binding and sensor specificity of FarR, a novel TetR family regulator required for induction of
627 the fatty scid efflux pump FarE in *Staphylococcus aureus*. J Bacteriol 201 (3):e00602-18.

628 52. Deutsch DR, Utter B, Verratti KJ, Sichtig H, Tallon LJ, Fischetti VA. 2018. Extra-chromosomal
629 DNA sequencing reveals episomal prophages capable of impacting virulence factor
630 expression in *Staphylococcus aureus*. Front Microbiol 9:1406.

631 53. Astorg P, Bertrais S, Laporte F, Arnault N, Estaquio C, Galan P, Favier A, Hercberg S. 2008.
632 Plasma n-6 and n-3 polyunsaturated fatty acids as biomarkers of their dietary intakes: a
633 cross-sectional study within a cohort of middle-aged French men and women. Eur J Clin Nutr
634 62:1155-61.

635 54. Hodson L, Skeaff CM, Fielding BA. 2008. Fatty acid composition of adipose tissue and blood
636 in humans and its use as a biomarker of dietary intake. Prog Lipid Res 47:348-80.

637 55. Al-Daghri NM, Torretta E, Barbacini P, Asare H, Ricci C, Capitanio D, Guerini FR, Sabico SB,
638 Alokail MS, Clerici M, Gelfi C. 2019. Sphingolipid serum profiling in vitamin D deficient and
639 dyslipidemic obese dimorphic adults. Sci Rep 9(1):16664.

640 56. Trinder M, Walley KR, Boyd JH, Brunham LR. 2020. Causal inference for genetically
641 determined levels of high-density lipoprotein cholesterol and risk of infectious disease.
642 Arterioscler Thromb Vasc Biol 40:267-278.

643 57. Dobner J, Kaser S. 2018. Body mass index and the risk of infection - from underweight to
644 obesity. Clin Microbiol Infect 24:24-28.

645 58. Lopez MS, Tan IS, Yan D, Kang J, McCreary M, Modrusan Z, Austin CD, Xu M, Brown EJ. 2017.
646 Host-derived fatty acids activate type VII secretion in *Staphylococcus aureus*. Proc Natl Acad
647 Sci U S A 114:11223-11228.

648 59. Nguyen MT, Luqman A, Bitschar K, Hertlein T, Dick J, Ohlsen K, Broker B, Schittek B, Gotz F.
649 2018. Staphylococcal (phospho)lipases promote biofilm formation and host cell invasion. Int
650 J Med Microbiol 308:653-663.

651 60. Jimenez-Dalmaroni MJ, Radcliffe CM, Harvey DJ, Wormald MR, Verdino P, Ainge GD, Larsen
652 DS, Painter GF, Ulevitch R, Beutler B, Rudd PM, Dwek RA, Wilson IA. 2015. Soluble human
653 TLR2 ectodomain binds diacylglycerol from microbial lipopeptides and glycolipids. Innate
654 Immun 21:175-93.

655 61. Rohmer C, Wolz C. 2021. The role of *hlb*-converting bacteriophages in *Staphylococcus aureus*
656 host adaption. Microb Physiol 31(2):109-122.

657 62. Ferlazzo AM, Bruschetta G, Di Pietro P, Medica P, Notti A, Rotondo E. 2011. Phospholipid
658 composition of plasma and erythrocyte membranes in animal species by 31P NMR. Vet Res
659 Commun 35:521-30.

660 63. Zardini Buzatto A, Abdel Jabar M, Nizami I, Dasouki M, Li L, Abdel Rahman AM. 2021.
661 Lipidome alterations induced by cystic fibrosis, CFTR mutation, and lung function. J Proteome
662 Res 20:549-564.

663 64. Fey PD, Endres JL, Yajjala VK, Widhelm TJ, Boissy RJ, Bose JL, Bayles KW. 2013. A genetic
664 resource for rapid and comprehensive phenotype screening of nonessential *Staphylococcus*
665 *aureus* genes. mBio 4:e00537-12.

666 65. Herbert S, Ziebandt AK, Ohlsen K, Schafer T, Hecker M, Albrecht D, Novick R, Gotz F. 2010.
667 Repair of global regulators in *Staphylococcus aureus* 8325 and comparative analysis with
668 other clinical isolates. Infect Immun 78:2877-89.

669 66. Pathania A, Anba-Mondoloni J, Gominet M, Halpern D, Dairou J, Dupont L, Lamberet G, Trieu-
670 Cuot P, Gloux K, Gruss A. 2021. (p)ppGpp/GTP and malonyl-CoA modulate *Staphylococcus*
671 *aureus* adaptation to FASII antibiotics and provide a basis for synergistic bi-therapy. mBio
672 12:e03193-20.

673 67. Katayama Y, Zhang HZ, Hong D, Chambers HF. 2003. Jumping the barrier to beta-lactam
674 resistance in *Staphylococcus aureus*. J Bacteriol 185:5465-72.

675